

# Earth's Future

## RESEARCH ARTICLE

10.1029/2020EF001611

### Key Points:

- We compared the life-cycle costs of groundwater pumping systems for irrigation powered by solar and diesel energy in sub-Saharan Africa
- Solar energy provides a more cost-effective energy solution to power groundwater irrigation in sub-Saharan Africa under many circumstances
- Investment in solar irrigation is subject to risk from uncertain future diesel prices; crops planted are also a key decision determinant

### Supporting Information:

Supporting Information may be found in the online version of this article.

### Correspondence to:

H. Xie,  
h.xie@cgiar.org

### Citation:

Xie, H., Ringler, C., & Hossain Mondal, M. A. (2021). Solar or diesel: A comparison of costs for groundwater-fed irrigation in sub-Saharan Africa under two energy solutions. *Earth's Future*, 9, e2020EF001611. <https://doi.org/10.1029/2020EF001611>

Received 5 MAY 2020

Accepted 18 JAN 2021

© 2021. The Authors. Earth's Future published by Wiley Periodicals LLC on behalf of American Geophysical Union. This is an open access article under the terms of the [Creative Commons Attribution License](https://creativecommons.org/licenses/by/4.0/), which permits use, distribution and reproduction in any medium, provided the original work is properly cited.

# Solar or Diesel: A Comparison of Costs for Groundwater-Fed Irrigation in Sub-Saharan Africa Under Two Energy Solutions

Hua Xie<sup>1</sup> , Claudia Ringler<sup>1</sup> , and Md. Alam Hossain Mondal<sup>1,2</sup>

<sup>1</sup>Environment and Production Technology Division, International Food Policy Research Institute, Washington, DC, USA, <sup>2</sup>Department of Electrical and Electronic Engineering, Daffodil International University, Dhanmondi, Dhaka, Bangladesh

**Abstract** Sub-Saharan Africa has long been beset with food insecurity and energy poverty. Expanding irrigated agriculture can help boost food production in the region, but this requires energy for accessing water, especially in groundwater-fed irrigation. This paper compared economic performance of groundwater pumping for irrigation under two energy solutions: solar photovoltaic (PV) and diesel fuel. We estimated the life-cycle costs of the power units of two pumping systems for a range of crop and irrigation method scenarios and mapped their relative cost-effectiveness over cropland in sub-Saharan Africa. As a renewable and clean energy source, solar energy has attracted much attention and there is keen interest in investing in solar PV to support the development of irrigated agriculture. Results of this study provide insights into the prospects of promoting solar irrigation in sub-Saharan Africa.

## 1. Introduction

Sub-Saharan Africa, a region of 23 million km<sup>2</sup> and home to more than 1 billion people, has long been beset with food insecurity (FAO & ECA, 2018). This situation can be largely attributed to the suboptimal performance of its agricultural sector and is correlated with underdeveloped irrigated agriculture in the region. Currently, only 5% of cropland in sub-Saharan Africa is equipped with irrigation (FAO, 2016), much less than any other developing region in the world. Lack of irrigation leaves crop production in sub-Saharan African countries susceptible to climate variability and limits production in the dry season. Boosting agricultural production through the development of irrigated agriculture is considered to be a promising option for addressing food insecurity (J. A. Burney et al., 2013; de Fraiture & Giordano, 2014; Xie et al., 2014).

This study maps the relative cost-effectiveness of groundwater-fed irrigation in sub-Saharan Africa under two off-grid energy solutions: solar photovoltaic (PV) and diesel fuel. Groundwater plays an important role in global irrigated agriculture. It is estimated that groundwater-fed irrigation accounts for about 40% of the global area equipped with irrigation (Siebert et al., 2010). The success of groundwater-fed irrigation in other regions suggests that groundwater may also be key to the development of irrigated agriculture in sub-Saharan Africa (Cobbing & Hiller, 2019; Villholth, 2013).

As groundwater irrigation requires energy to lift water, the cost and efficiency of the energy technology are key determinants of the performance of the irrigation system (Belaud et al., 2020; Langarita et al., 2017; Tarjuelo et al., 2015). Various energy solutions are available for water pumping. In this study we chose to focus on diesel and solar energy since these are the two most promising off-grid solutions to powering groundwater-fed irrigation in sub-Saharan Africa. The analysis can be extended in the future to include other options such as on-grid electric pumps and manual treadle pumps. However, the potential applicability of the former is restricted by the current low access to the electric grid in sub-Saharan Africa (Blimpo & Cosgrove-Davies, 2019) and use of the latter is hampered by labor-intensity and gender inequity (Njuki et al., 2014).

Compared to diesel, solar energy is an emerging energy technology whose application to power-irrigated agriculture has been attracting much attention in recent years (Hartung & Pluschke, 2018). Various studies have compared the costs of using these two energy technologies for irrigation water pumping at site scale (Girma et al., 2015; Hossain et al., 2015; Kelley et al., 2010; Lorenzo et al., 2018). This study is designed to

**Table 1**  
*Crop Irrigation-Method Scenarios*

Scenario	Crop	Irrigation method
1	Maize	Flood
2	Wheat	Flood
3	Tomatoes	Drip
4	Tomatoes	Flood
5	Onions	Drip
6	Onions	Flood
7	Chickpeas	Drip
8	Chickpeas	Flood
9	Common beans	Drip
10	Common beans	Flood
11	Sugarcane	Flood
12	Bananas	Flood

provide a cost comparison analysis at regional level and to map the relative cost-effectiveness of groundwater pumping for irrigation powered by solar PV and diesel energy over the entire sub-Saharan Africa region. Specifically, we compared the costs of solar powered groundwater irrigation and diesel irrigation site-by-site across sub-Saharan Africa under a number of crop and irrigation method scenarios. In each scenario, an irrigated crop type as well as an irrigation method are assumed within the production suitability domain of the crop and with flood and drip as alternative irrigation methods. The results of the analysis allow us to examine the spatial and across-crop variability of the economic performance of the two energy solutions in pumping groundwater for irrigation and can be used to inform policy discussions on the role these solutions may play in supporting future development of groundwater-fed irrigated agriculture. Szabó et al. (2011) compared the costs of electrification by distributed solar and diesel generation in Africa, using a presumed residential energy consumption pattern. The pattern of energy demand for irrigation water pumping, however, varies with climate and also by crop and irrigation method and could differ substantially from that of residential use. There is therefore a need for a separate study identifying cost-effective energy solutions for irrigation.

The rest of the paper is organized as follows. Section 2 describes the crop-irrigation method scenarios and other key settings of the analysis. Section 3 presents the data and method we used to size pumping systems under two energy solutions and estimate their life-cycle costs. The results of the cost comparison analysis are presented in Section 4, which is followed by a concluding section where implications of findings of the study and direction for future research are further discussed.

## 2. Crop-Irrigation Method Scenarios, Boundary of Pumping System for Life-Cycle Cost Estimation and Spatial Extent of the Comparison Analysis

The crop irrigation-method scenarios we used are shown in Table 1. They were formulated to represent possible typical combinations of crops and irrigation technologies. Case studies, although limited, have shown that farmers are more likely to use irrigation to cultivate high-value crops (see a review in Domènech, 2015). In this study, we included vegetables, pulses, sugarcane, maize, wheat, and fruits; we selected tomatoes and onions as representative vegetable crops, chickpeas and common beans as representative pulse crops, and banana as a representative fruit crop.

In terms of irrigation methods, flood and drip irrigation are two ends of a broad spectrum of irrigation methods, where flood irrigation is characterized by a low field application efficiency and drip by a high application efficiency. Drip irrigation has been promoted substantially in sub-Saharan Africa over the past 2 decades, and specifically low-cost drip (J. Burney et al., 2010; Postel et al., 2001; Woltering et al., 2011). Our scenarios consider the use of low-cost drip for the cultivation of tomatoes, onions, chickpeas, and common beans.

Most areas in sub-Saharan Africa have a tropical climate with alternating rainy and dry seasons, the latter with a more intensive water and energy requirement for irrigation. In carrying out the analysis, we use the dry season irrigation energy demand to define the size and operational costs of water pumping systems.

The costs in this study refer to the life-cycle costs of solar and diesel water pumping systems. The life-cycle cost of a water pumping system consists of capital costs, operation and maintenance costs (O&M), fuel costs, and replacement costs (World Bank, 2018). We did not consider nonfinancial costs associated with environmental externalities, such as reduced greenhouse gas emissions. To simplify the analysis, the system boundary is defined to include the power unit only by assuming the same costs for motor and pumps (Abu-Aligah, 2011; Kelley et al., 2010). Moreover, although the study is not designed to score the environmental suitability of groundwater-fed irrigation, GIS layers indicating sites with favorable conditions for

Category	Inclusion criteria	Data source
Cropland extent	Cropland percentage > 0	1 km global IIASA-IFPRI cropland percentage map (Fritz et al., 2015)
Slope	<8%	Shuttle Radar Topography Mission (SRTM) digital elevation data
Groundwater depth	<50 m	British Geological Survey digital groundwater maps of Africa (MacDonald et al., 2012)
Groundwater productivity	>0.1 l/s	British Geological Survey digital groundwater maps of Africa (MacDonald et al., 2012)
Agro-climatically attainable yield	>0 under irrigation	IIASA-FAO Global Agro-ecological Zones (GAEZ) (Fischer et al., 2012)

groundwater-fed irrigated production for each crop were determined using criteria shown in Table 2. We limited the analysis to the spatial extent of these suitability domains.

### 3. Data and Methods for Life-Cycle Cost Estimation

The procedure for estimating cell-wise values of life-cycle costs of solar PV- and diesel-powered groundwater irrigation pumping systems is schematically shown in Figure 1, with key input parameters and calculated variables listed. It follows the same logic applied in reported single-site economic studies on solar/diesel water pumping systems. However, the very large spatial scale of the analysis in this study has implication for choosing the calculation approach used in each step of the estimation. Implementation details of the life-cycle cost estimation procedure are explained below. All spatial input data were resampled to a resolution of 0.0083 latitude-longitude degree (~1 km) in the analysis and the results are reported at that resolution.

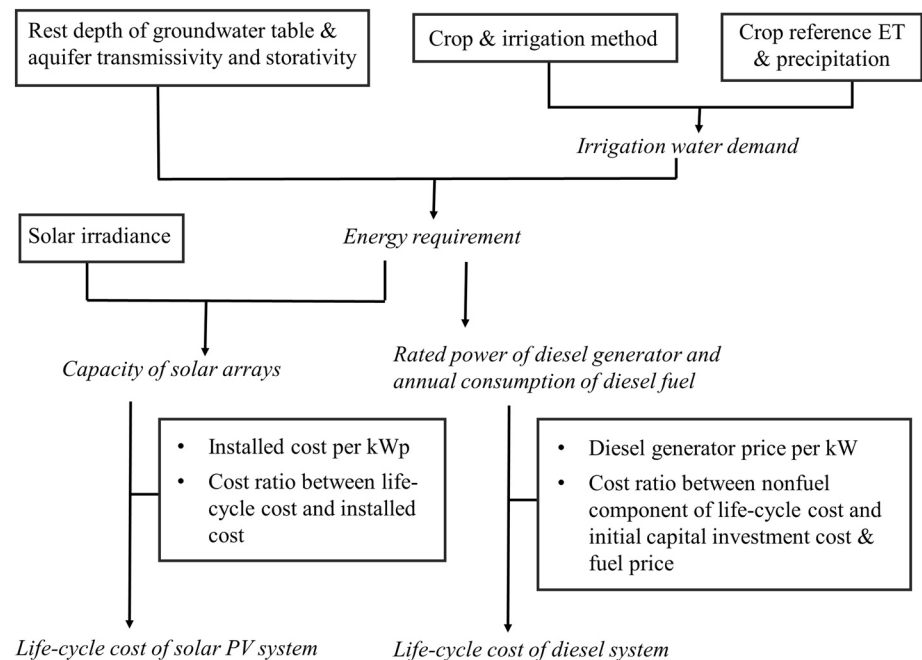


**Figure 1.** Estimation procedure of life-cycle costs of solar PV and diesel water pumping systems for groundwater-fed irrigation. Names of input variables/parameters are shown in the rectangle. Names of calculated variables appear in italic.

### 3.1. Solar PV and Diesel Power System Sizing

To inform the estimation of system-wide life cycle costs, we first sized power units of pumping systems under two energy solutions. The size of a solar PV array, which is rated by electricity generation capacity under standard testing conditions (STC) in kilowatts peak (kWp), is estimated as:

$$P_{\text{array\_STC}} = \max \{ E_i / (h_i \cdot df) \} \quad (1)$$

where  $P_{\text{array\_STC}}$  is the rated power of the solar array under standard testing conditions (kWp), subscript  $i$  denotes the month in the growing season,  $E_i$  is the daily mean energy requirement for irrigation in month  $i$  (kWh),  $h_i$  is the peak sun hour (hr) in month  $i$ , and  $df$  is a derating factor.

The peak sun hour at a location is numerically identical to the daily solar insolation received at that location, measured in units of kWh/m<sup>2</sup>. The average daily solar insolation over sub-Saharan Africa in each month was calculated from solar irradiance data obtained from the Photovoltaic Geographical Information System (PVGIS)'s Satellite Application Facility on Climate Monitoring (CM SAF) database between 2005 and 2015 (Huld et al., 2012).

The derating factor,  $df$ , is a coefficient that is included in order to account for the reduction in electricity output caused by various factors such as temperature, dirt, and wiring loss. As data to estimate the derating factor are not available for the entire study area, a constant value of 0.77 is assumed in this analysis; this default value is typically used when no further estimates are available (World Bank, 2018).

To estimate the energy requirement  $E_i$ , we first calculated crop-irrigation water demand using the FAO-56 approach (Allen et al., 1998). The daily mean net irrigation water demand in month  $i$  is calculated as

$$D_{\text{net},i} = (ET_{0,i} \cdot k_{c,i} - P_{\text{eff},i}) / \text{ndays}_i \quad (2)$$

where  $D_{\text{net},i}$  is the daily mean net irrigation water demand in month  $i$  expressed in depth of water (mm H<sub>2</sub>O),  $ET_{0,i}$  is the monthly reference evapotranspiration (mm H<sub>2</sub>O),  $k_{c,i}$  is the crop coefficient in month  $i$ ,  $P_{\text{eff},i}$  is the effective rainfall in month  $i$  (mm H<sub>2</sub>O), and  $n \text{ days}_i$  is the number of days in month  $i$ .

Effective rainfall,  $P_{\text{eff},i}$ , is estimated by using the method proposed by the US Department of Agriculture Soil Conservation Service (Smith, 1992):

$$P_{\text{eff},i} = \frac{P_i (125 - 0.2P_i)}{125} \text{ for } P_i \leq 250 \text{ mm / mo} \quad (3)$$

$$P_{\text{eff},i} = 125 + 0.1P_i \text{ for } P_i > 250 \text{ mm / mo}$$

where  $P_i$  is the monthly precipitation in month  $i$  (mm H<sub>2</sub>O).

Average crop reference evapotranspiration and precipitation by month,  $ET_{0,i}$  and  $P_i$ , are derived from time-series data of crop reference evapotranspiration and precipitation during the PVGIS solar irradiance data period from the CRU TS (v. 4.03) (Harris et al., 2014) and the CHIRPS (Funk et al., 2015) data set, respectively. The values of crop coefficients  $k_{c,i}$  used in this study are the monthly averages of daily  $k_c$  values from constructed  $k_c$ -crop growth stage curves (Allen et al 1998; also see Table S1 for more details).

The net irrigation demand is adjusted for application efficiency of irrigation in order to yield an estimate of the gross irrigation water demand:

$$D_{\text{gross},i} = \frac{D_{\text{net},i}}{\eta_{\text{irr}}} \quad (4)$$

where  $D_{\text{gross},i}$  is the daily mean gross irrigation water demand in month  $i$  (mm H<sub>2</sub>O) and  $\eta_{\text{irr}}$  is the projected efficiency of irrigation. The application efficiency of flood irrigation in this study is assumed to be 0.5 (FAO, 1997) and the application efficiency of drip irrigation is set to 0.9 (Brouwer et al., 1989).

With estimated irrigation water demand, the daily average energy requirement for irrigation water pumping in month  $i$ ,  $E_i$ , is calculated as

$$E_i = \frac{D_{\text{gross},i} \cdot A \cdot 10 \cdot \rho \cdot g \cdot H}{3.6 \times 10^6 \cdot \eta} \quad (5)$$

where  $A$  is farm size or irrigated area in hectares (ha), 10 is a factor used to calculate the conversion of gross irrigation demand (expressed in mm H<sub>2</sub>O) to gross irrigation water demand in cubic meters (m<sup>3</sup> H<sub>2</sub>O),  $\rho$  is the density of water (in 1,000 kg/m<sup>3</sup>),  $g$  is the gravity of the Earth (9.8 m / s<sup>2</sup>),  $H$  is the total dynamic head (m),  $\eta$  is the energy efficiency of the motor and the pump, and  $3.6 \times 10^6$  is the conversion factor from joules to kWh.

The total dynamic head,  $H$ , consists of elevation head, pressure head, and friction loss. Elevation head is the vertical distance from the groundwater table to the ground surface. It further comprises the depth of the rest groundwater table and the drawdown caused by pumping. The drawdown variation in each pixel in this study was estimated by using the analytical solution of the single-well model which is proposed to simulate the water table response to pumping in individual boreholes. This approach has the limitation of omitting groundwater table variations that are caused by interactions between the cone depression of the borehole of interest and the cone depressions of other boreholes which may be located nearby, and interactions between boreholes and nearby natural surface waterbodies. The use of this approach also implicitly assumes that the groundwater table can fully recover during the rainy season. However, it provides a computationally economical method with parsimonious input data requirements to contribute to the pumping height estimation in large-scale groundwater resources planning analysis (Bonsor & MacDonald, 2011; MacDonald et al., 2009). Specifically, in this study the drawdowns at the end of each month during the growing season are calculated by applying the Theis equation (Theis, 1935) and the principle of superposition in time:

$$H_s = \frac{Q_1}{4\pi T} W(u_1) + \frac{Q_2 - Q_1}{4\pi T} W(u_2) + \frac{Q_3 - Q_2}{4\pi T} W(u_3) + \dots$$

$$W(u_n) = -0.5772 - \ln(u_n) + u_n - \frac{u_n^2}{2 \times 2!} + \frac{u_n^3}{3 \times 3!} - \frac{u_n^4}{4 \times 4!} + \dots \quad n = 1, 2, 3, \dots \quad (6)$$

$$u_n = \frac{r^2 S}{4Tt_n} \quad n = 1, 2, 3, \dots$$

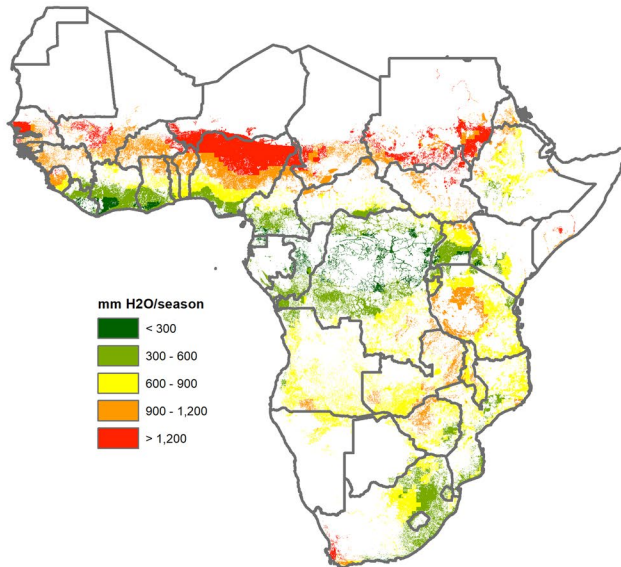
where  $H_s$  is the drawdown (m),  $Q_n$  ( $n = 1, 2, 3, \dots$ ) is the pumping rate in the  $n$ th month  $i$  (m<sup>3</sup>/d; =  $D_{\text{gross},n} \cdot A \cdot 10$ ),  $T$  is transmissivity (m<sup>2</sup>/d),  $S$  is storativity (dimensionless),  $r$  is the distance to the center of the borehole and denotes the radius of the borehole,  $t_n$  is the elapsed time since pumping rate  $Q_n$  starts (d).

Estimates for depth of natural or rest groundwater level are obtained from digital groundwater depth maps of Africa developed by the British Geological Survey (BGS) (MacDonald et al., 2012). The estimated rest groundwater table depth on this map falls into six classes: very shallow: 0–7 m; shallow: 7–25 m; shallow to moderate: 25–50 m; moderate: 50–100 m; deep: 100–250 m; and very deep: >250 m. A study in Tanzania (Baumann et al., 2005) indicates that the average rest groundwater table depth for boreholes over all 20 regions in Tanzania is about 17 m, but in some regions the average rest groundwater table depth exceeds 30 m. In this study, we assumed that groundwater-fed irrigation may occur at locations with a rest groundwater depth of up to 50 m, that is, within the first three groundwater depth classes of the BGS groundwater depth map (Table 2).

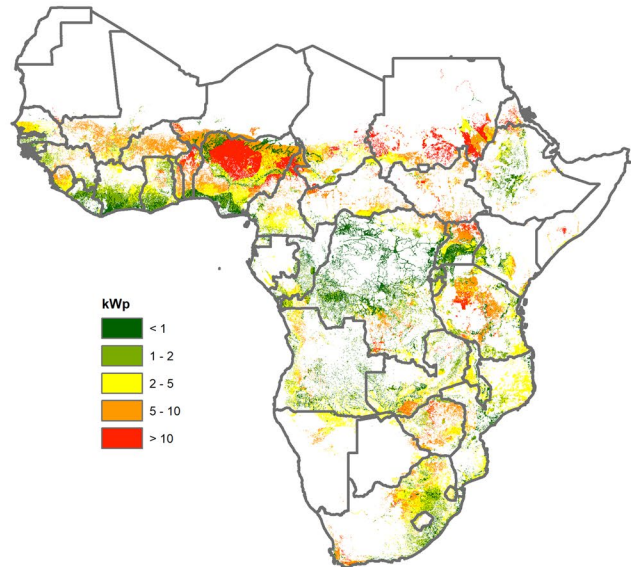
In applying Equation 6 for the drawdown estimation, the borehole radius is assumed to be 0.075 m or 3 inches (BWA, 2020). Values used for storativity  $S$  are suggested by de Graaf et al. (2017) and are assigned according to lithology classes defined by Hartmann and Moosdorf (2012). Transmissivity  $T$  is the most sensitive parameter in Equation 6. Estimates of transmissivity are derived from the aquifer productivity map in BGS' digital groundwater maps of Africa (MacDonald et al., 2012). The BGS aquifer productivity map shows spatial distributions of six aquifer productivity classes, and ranges of estimated transmissivity  $T$  corresponding to each aquifer productivity class are provided by Bonsor and MacDonald (2011): 500–1,000 m<sup>2</sup>/d for aquifers with very high productivity (>20 l/s), 50–500 m<sup>2</sup>/d for aquifers with high productivity (5–20 l/s), 10–50 m<sup>2</sup>/d for aquifers with moderate productivity (1–5 l/s), 5–10 m<sup>2</sup>/d for aquifers with low to moderate productivity (0.5–1 l/s) and 1–5 m<sup>2</sup>/d for aquifers with low productivity (0.1–0.5 l/s). Aquifers with very



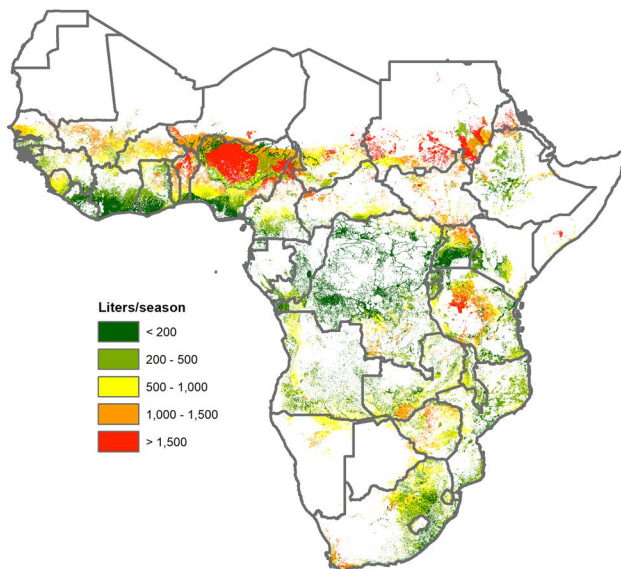
(a) Gross irrigation water demand



(b) Size of solar PV system



(c) Consumption of diesel fuel



(d) Power of diesel generator

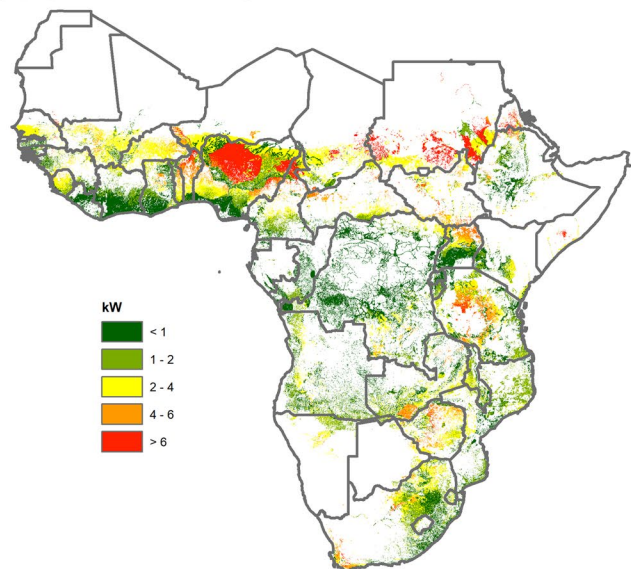


**Figure 2.** Expected values of seasonal irrigation water demand, diesel fuel consumption and required capacity of the solar PV system and power of the diesel generator derived from the Monte Carlo-based sizing calculation under the tomatoes + flood irrigation scenario.

low productivity ( $<0.1$  l/s) are considered not suitable for developing groundwater irrigation (Schmitter et al., 2018) and thus are excluded from this cost comparison analysis (Table 2).

As the estimates for rest groundwater depth and transmissivity  $T$  are provided as categorical data and the wide ranges of values of the two parameters in each class, Monte Carlo simulations were conducted. Samples of the two parameters were randomly drawn by assuming uniform distributions over value ranges of groundwater depth and transmissivity classes. The expected values of energy requirements  $E_i$  calculated from the Monte Carlo simulation are used in the ensuing calculations.

Pressure head in total dynamic head is zero in flood irrigation and is assumed to be 2 m in low cost drip irrigation systems (Phocaides, 2007). Friction loss is assumed to be 10% of the elevation head (World Bank, 2018).

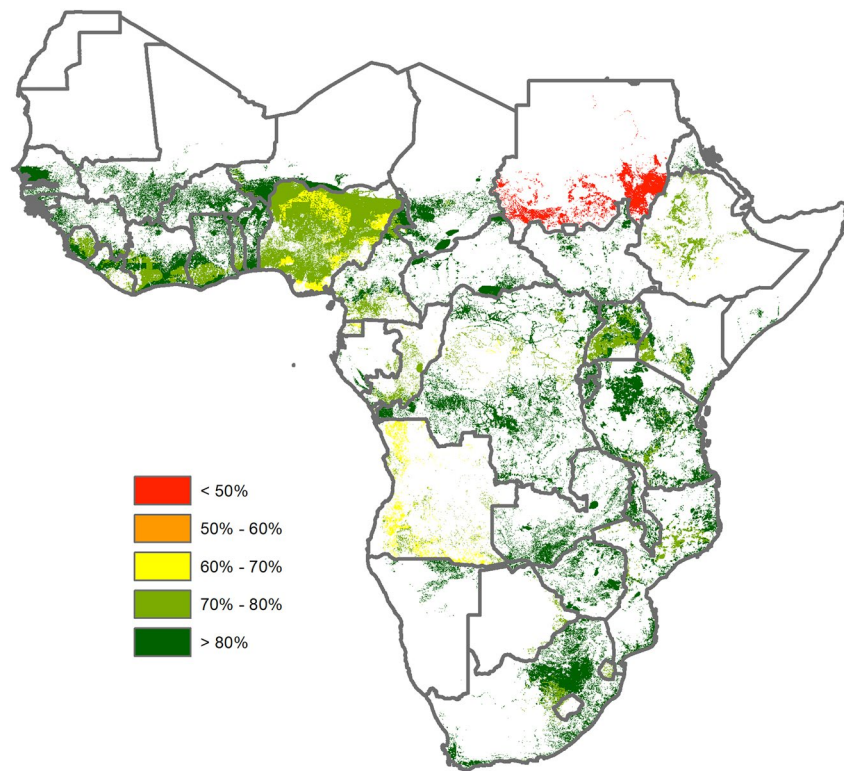
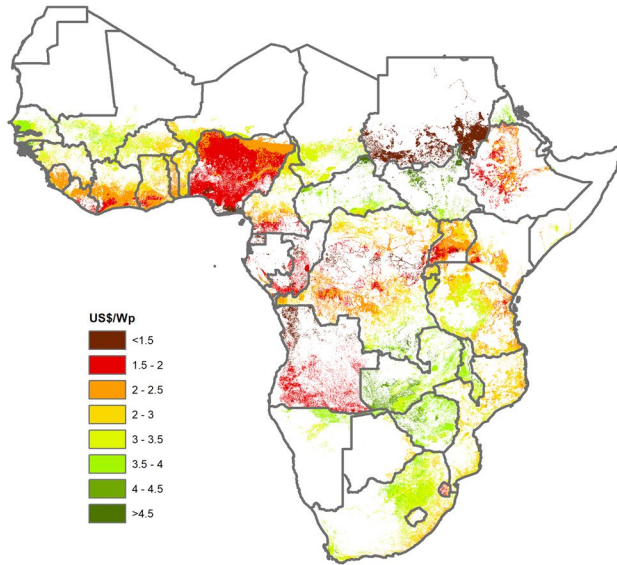


**Figure 3.** Percentage share of fuel cost in life-cycle cost of the diesel power system under the tomatoes + flood irrigation reference diesel fuel price scenario.

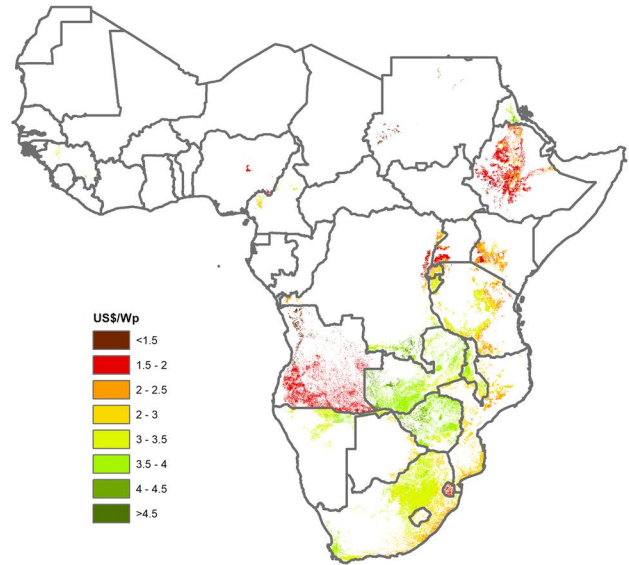
The energy requirement in Equation 5 also depends on the energy efficiency of motor and pump,  $\eta$ , and farm size,  $A$ .  $\eta$  is set to 0.6 (Kelley et al., 2010; Phocaides, 2007). In sub-Saharan Africa, small farms dominate (FAO 2020; Fritz et al 2015; Lowder et al 2016). However, detailed information on farm size distribution is lacking. Because of this, farm size was also considered as an uncertain parameter and included in the Monte Carlo simulation, together with rest groundwater depth and transmissivity  $T$ . A uniform distribution was assumed for farm size variable. The upper limit of farm size was set to 2 hectares or the maximum irrigated area which can be supported by a single borehole, if such maximum irrigated area calculated according to the irrigation water demand and borehole yield from BGS aquifer productivity map is less than 2 hectares.

As a remark on the sizing approach for solar PV systems noted above, monthly solar irradiance, crop reference evapotranspiration and precipitation data are used in the sizing calculations. Site-scale case studies of applying this method to size solar PV water pumping systems for irrigation are reported by Cuadros et al. (2004) and Barrueto Guzmán et al. (2018). Some authors consider this method to be more appropriate for the preliminary design of solar PV systems, which could be followed by a more detailed design analysis that involves simulations of the solar irradiance–electricity production relationship at sub-daily timestep (Abu-Aligah, 2011; World Bank, 2018). In this study, the method with monthly time step of calculations was chosen due to the strategic planning nature of the analysis and the lack of site-specific data which are needed to support a more detailed sizing analysis. Moreover, a typical solar PV system sizing process also includes procedures to determine the specifications of other equipment/accessories in the system and optimizing the configuration of system. Correspondingly, life cycle cost analysis typically requires specifying the cost cash flows associated with each equipment in the system over their life spans as input (Short et al., 1995). In view of the fact that the solar array is the principal component of the solar PV system, a full design and configuration optimization of the solar PV system requires strong local knowledge and cost information on components of the solar PV system other than the solar array is even more scarce, in this study we chose to limit the sizing calculations to solar PV arrays and a variant method is implemented to estimate the life-cycle cost of the whole solar PV system: as indicated in the next section, we estimated the system-wide life-cycle cost of the solar PV pumping system by assuming that it varies in proportion to the installed cost of the solar array.

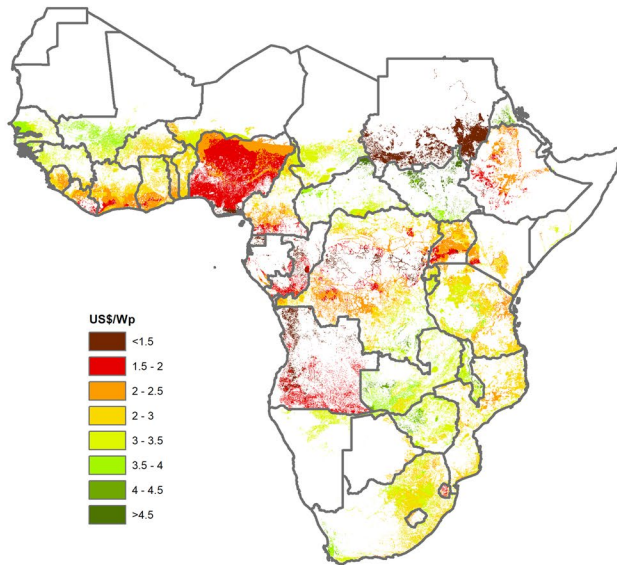
(a) Maize + flood irrigation



(b) Wheat + flood irrigation



(c) Tomatoes + drip irrigation



(d) Tomatoes + flood irrigation

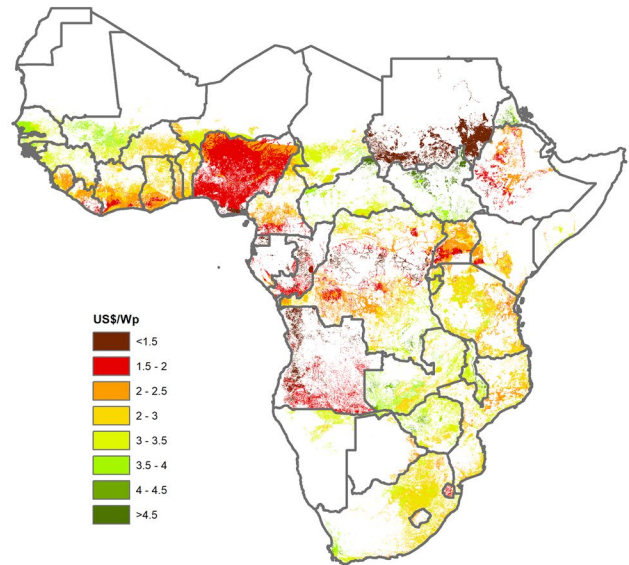


**Figure 4.** Breakeven installed cost of solar PV irrigation systems (Madagascar is not included in the analysis due to lack of groundwater depth data).

In the sizing of diesel pumping systems, we estimated the power of the diesel generators and the consumption of diesel fuel. The required power of a diesel generator  $P_{\text{gen}}$  (kW) is estimated as

$$P_{\text{gen}} = \frac{\max E_i}{h_{\text{diesel}}} \quad (7)$$

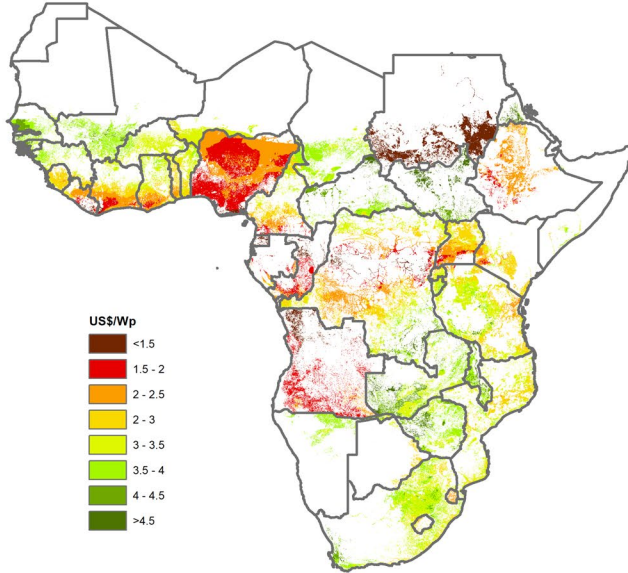
where  $\max E_i$  denotes the daily mean energy requirement in a peak month (kWh),  $h_{\text{diesel}}$  is daily operation hours (hr) which is set to 10 h in this study (EMCON, 2006).

The annual consumption of diesel through the whole growing season is calculated as

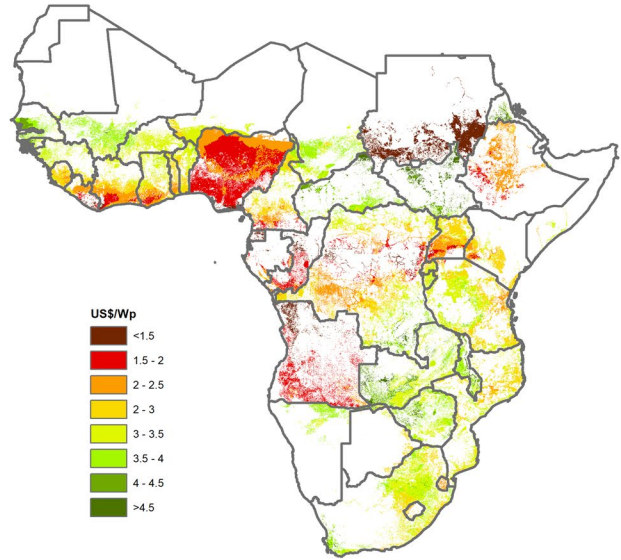
$$V = \frac{\sum_{i=1}^n E_i \cdot \text{ndays}_i}{e} \quad (8)$$



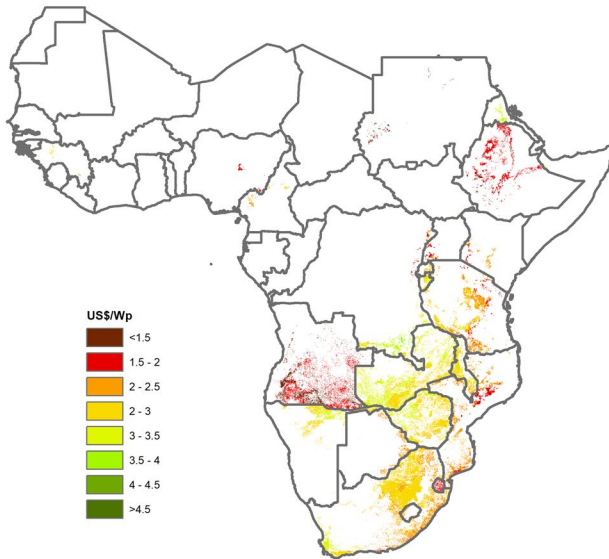
(e) Onions + drip irrigation



(f) Onions + flood irrigation



(g) Chickpeas + drip irrigation



(h) Chickpeas + flood irrigation

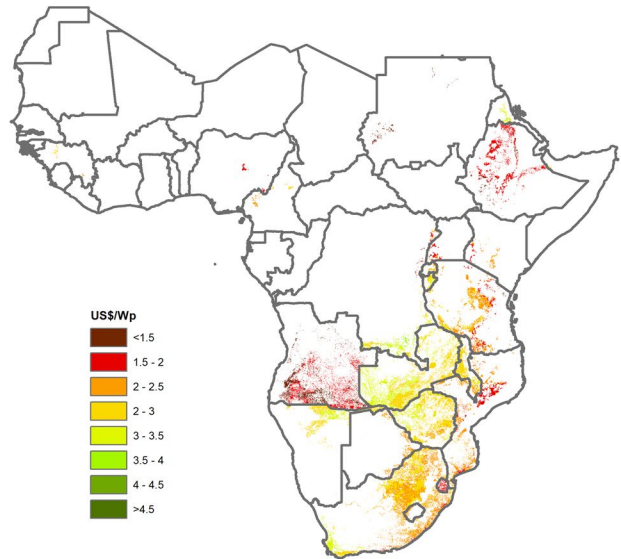


Figure 4. Continued

where  $V$  is the annual diesel consumption in liters (l),  $E_i$  is the calculated daily mean energy requirement (kWh) in month  $i$ ,  $ndays_i$  is the number of days in month  $i$ , and  $e$  is diesel consumption per kWh  $\approx 0.4$  l/kWh.

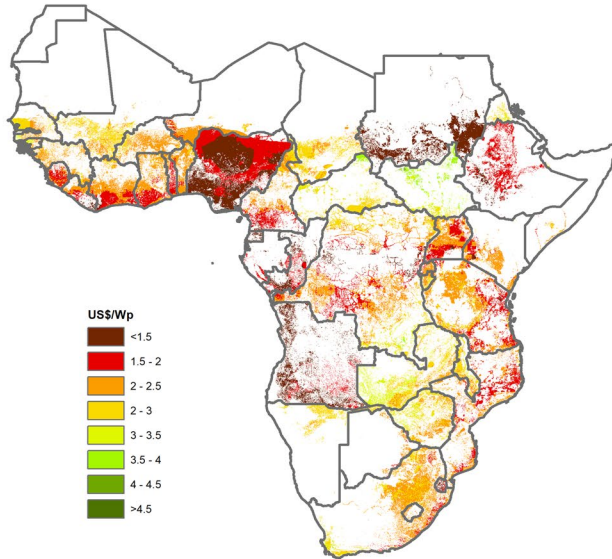
### 3.2. Life-Cycle Cost Estimation of Solar PV and Diesel Pumping Systems

Using the estimated rating of solar PV arrays and diesel generators and annual diesel fuel consumption, we estimated the present value of the life cycle cost of the two water lifting systems over a 25-year period, which is the typical life expectancy of a solar array and thus is often chosen as the assessment horizon.

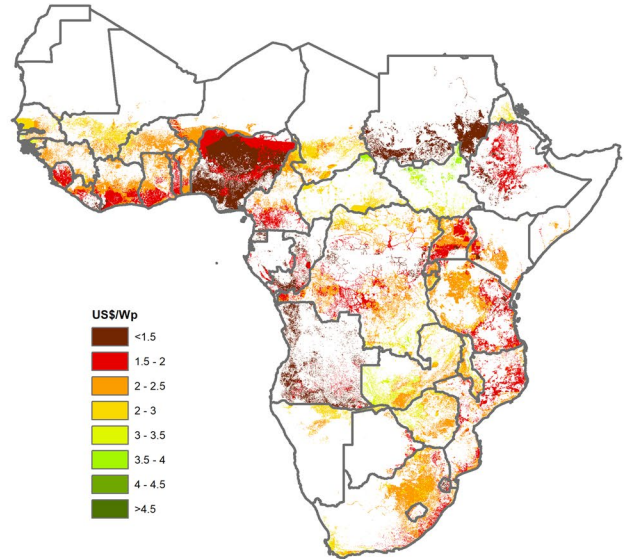
The life cycle cost of a power unit in solar PV pumping is calculated as

$$LCC_{\text{solar}} = 1000 \cdot P_{\text{array\_STC}} \cdot C_{\text{installed}} \cdot f_{\text{IC}} \quad (9)$$

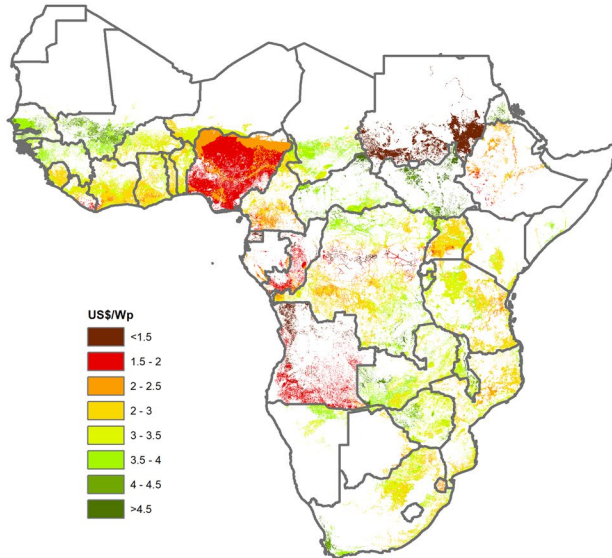
(i) Common beans + drip irrigation



(j) Common beans + flood irrigation



(k) Sugarcane + flood irrigation



(l) Banana + flood irrigation

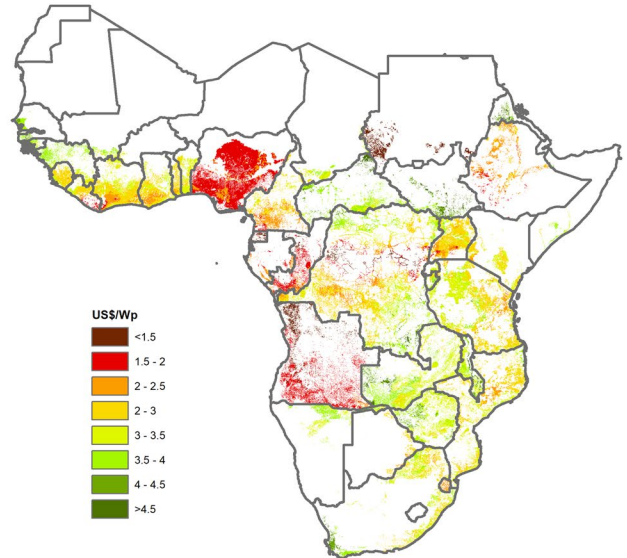


Figure 4. Continued

where  $LCC_{\text{solar}}$  is the present value of the life-cycle cost of the power unit of the solar PV water pumping system (US\$),  $P_{\text{array\_STC}}$  is the rated power of the solar array (kWp) calculated in Equation 1,  $C_{\text{installed}}$  is the installed cost of the solar array per watt peak (US\$/Wp),  $f_{\text{IC}}$  is an estimated ratio of the system-wide life-cycle cost to the total installed cost of the power unit.

The life cycle cost of the power unit in diesel water pumping systems is estimated as

$$LCC_{\text{diesel}} = GC_{\text{gen}} + FC_{\text{diesel}} \quad (10)$$

where  $LCC_{\text{diesel}}$  is the present value of the life-cycle cost of the power unit in diesel water pumping systems (US\$), and  $GC_{\text{gen}}$  is the present value of the nonfuel cost components through the span of the life-cycle assessment period (in US\$), which includes the cost of the diesel generator purchase, installation, maintenance, and replacement.  $FC_{\text{diesel}}$  is the present value of the diesel fuel costs over the life cycle of the pumping system (in US\$).

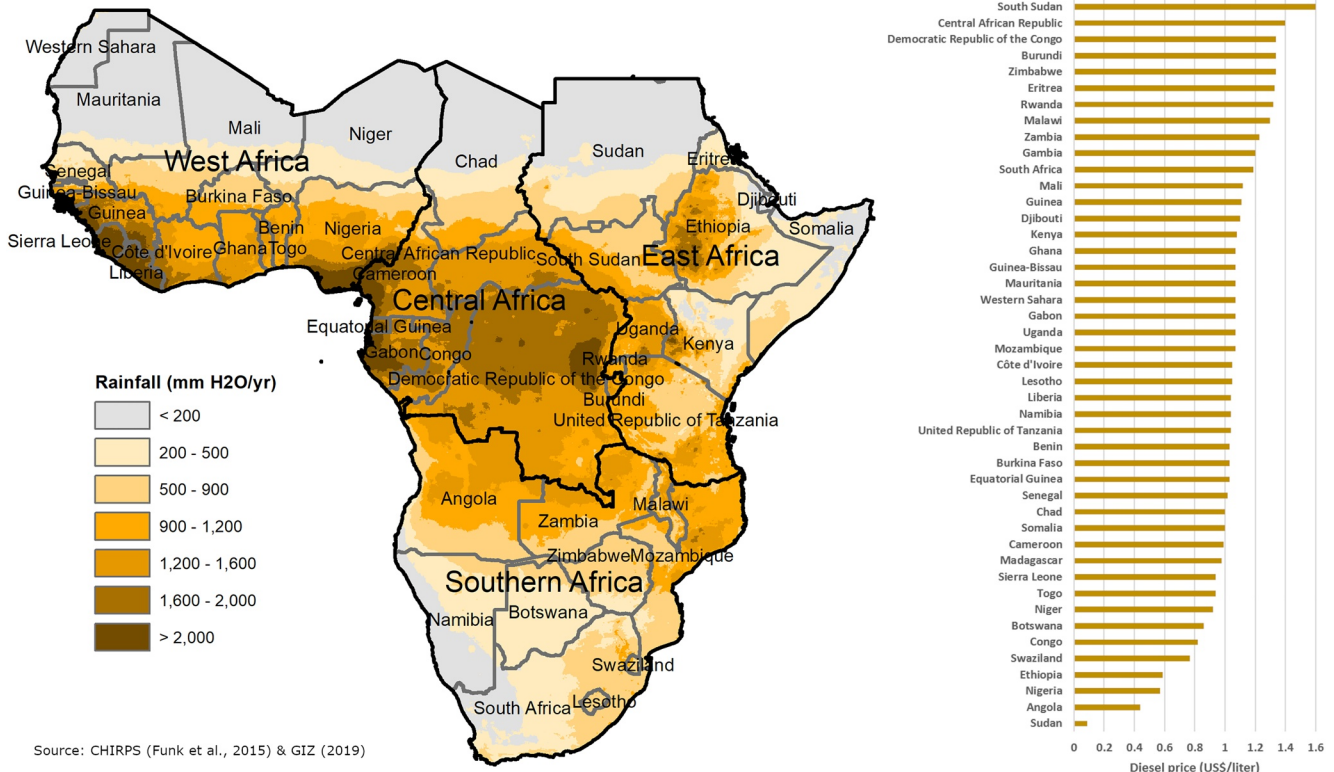


Figure 5. Climate and diesel prices in sub-Saharan African countries.

$GC_{gen}$  is calculated as

$$GC_{gen} = P_{gen} \cdot C_{gen} \cdot f_{gen} \quad (11)$$

where  $P_{gen}$  is the power rating of the diesel generator (kW),  $C_{gen}$  is the initial investment of purchasing and installing the diesel generator per kilowatt (US\$/kW),  $f_{gen}$  is the ratio coefficient between initial investment and the present value of total nonfuel costs.

The present value of the diesel fuel cost over the 25-year assessment period is calculated as

$$FC_{diesel} = \sum_{y=0}^{24} pr_{diesel} \cdot (1 + pe)^y \cdot V \cdot \frac{1}{(1 + d)^y} \quad (12)$$

where  $PV_{diesel}$  is the present value of the diesel fuel cost (US\$),  $y$  is the number of future years,  $pr_{diesel}$  is the diesel price (US\$/liter) in the base year or year 0,  $pe$  is the escalation rate of the diesel fuel price,  $V$  is the annual consumption of diesel fuel (liters), and  $d$  is the discount rate.

Apart from the variables calculated from the system sizing, the input data and the values of parameters used in the life-cycle cost estimation of the two systems are described below.

For the estimation of nonfuel costs in the life cycle of diesel power systems, the investment incurred in year zero is estimated by multiplying the rated power of the diesel generator in kilowatts by the unit investment cost of the diesel generator per kilowatt. The unit investment cost,  $C_{gen}$ , is set at US\$300/kW, which consists of an average price of US\$270/kW for equipment purchase - estimated using online dealer pricing information from selected sub-Saharan African countries (Kenya, Nigeria, and South Africa)—and an added installation cost which is assumed to be 10% of the cost of equipment purchase (Kelley et al., 2010). Diesel generators require maintenance such as oil, filter, and coolant changes, and regular replacement of parts. The interval of maintenance and replacement services depends on the quality of the equipment. Fulfilling the services requires



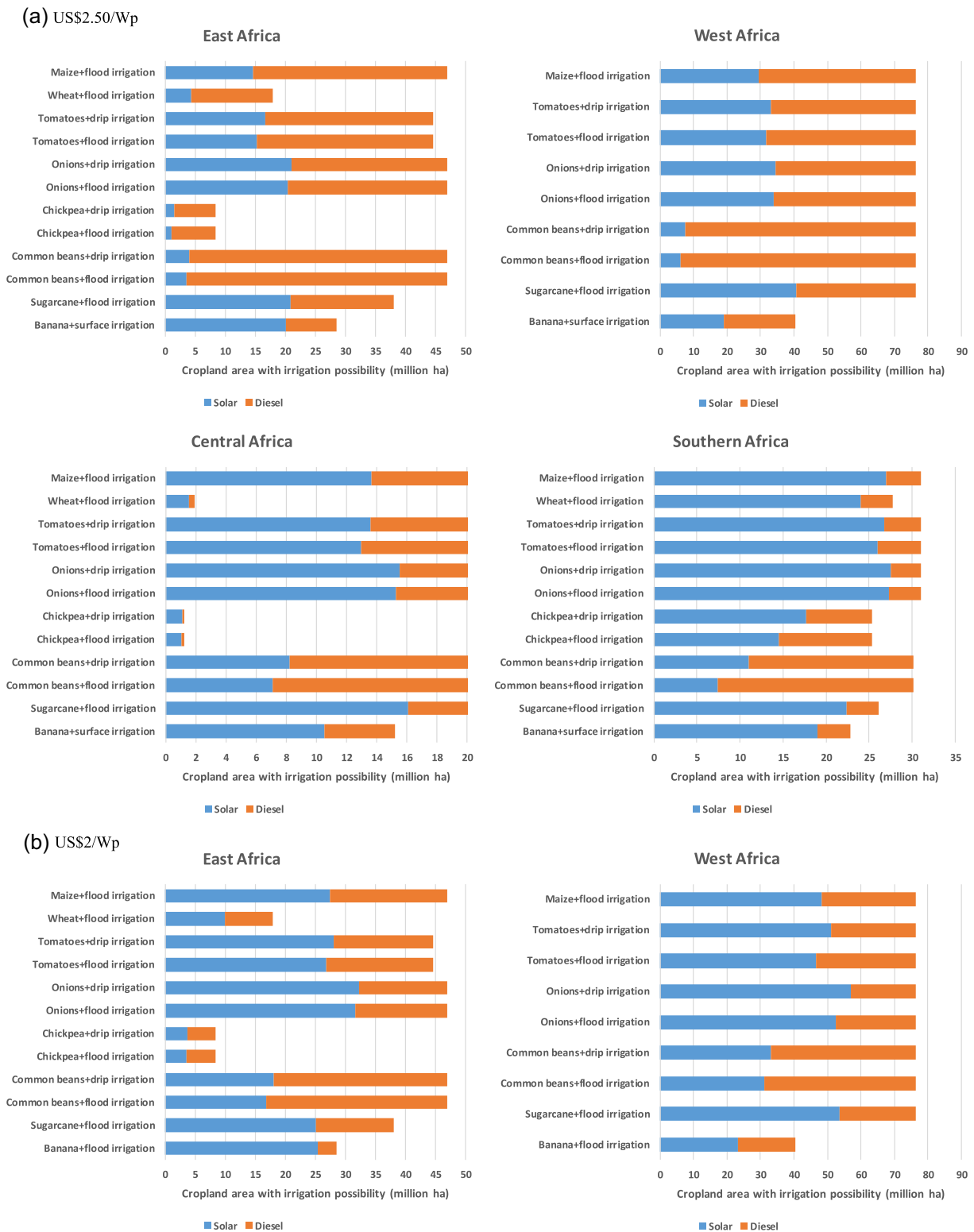


**Figure 6.** Cost-effective area under solar PV and diesel irrigation, under the reference scenario of diesel fuel pricing (escalation rate of 2%). East African countries include Eritrea, Ethiopia, Kenya, Rwanda, Somalia, Sudan, Tanzania, Uganda, and Djibouti; West African countries include Benin, Burkina Faso, Côte d'Ivoire, Ghana, Guinea, Guinea-Bissau, Liberia, Mali, Mauritania, Niger, Nigeria, Senegal, Sierra Leone, The Gambia, Togo and Western Sahara; Central African countries include Burundi, Cameroon, Central African Republic, Chad, Congo, Congo DRC, Equatorial Guinea and Gabon; Southern African countries include Angola, Botswana, Lesotho, Malawi, Mozambique, Namibia, South Africa, Swaziland, Zambia, and Zimbabwe. Areas of cropland suitable for wheat and chickpea production in West Africa are very small and are not shown in the charts. For results on these two crops, refer to the Excel source data file in the supporting information.



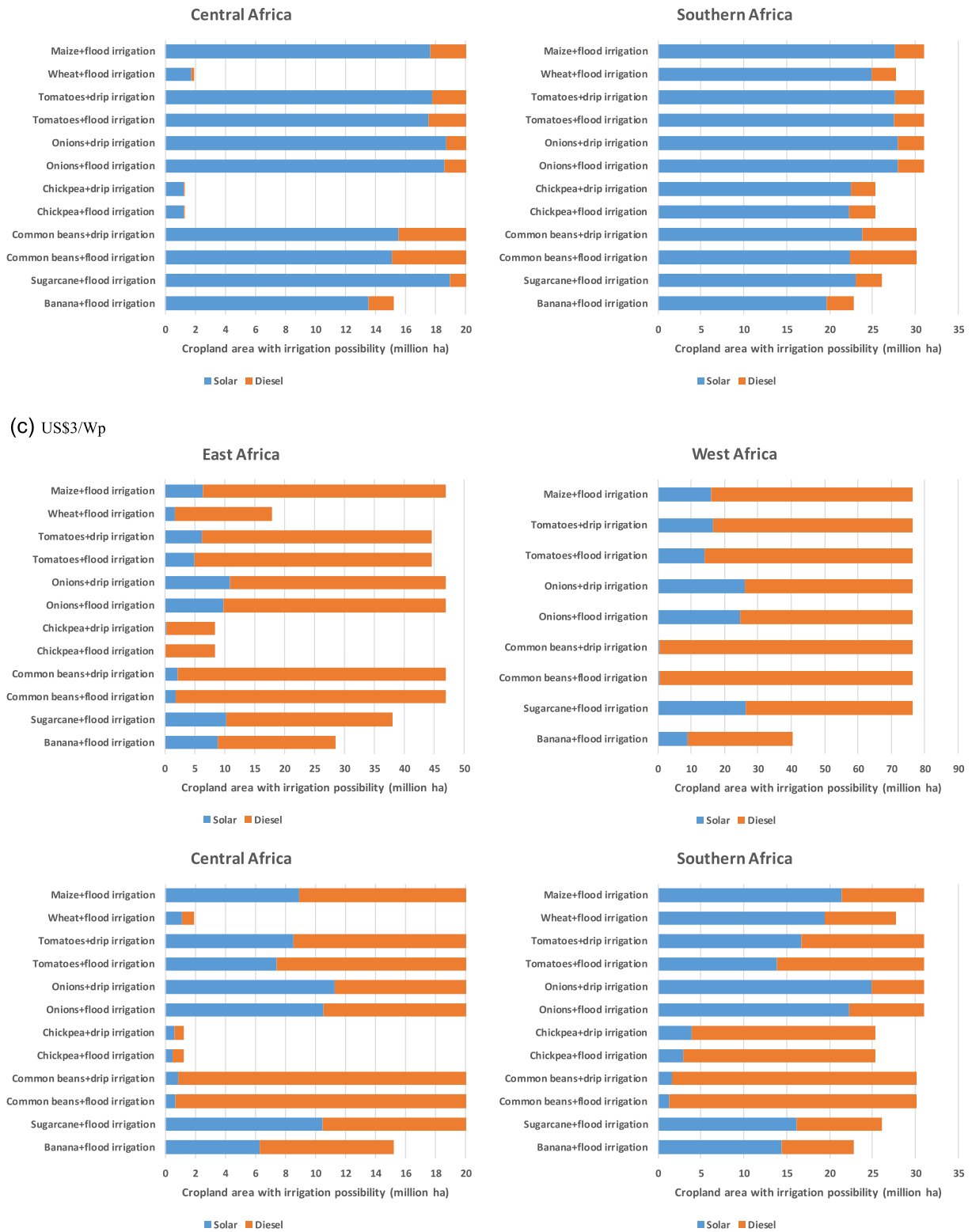


Figure 6. Continued

skilled workers and therefore incurs substantial labor costs. Without site-by-site data available for determining the maintenance costs, a factorial approach is taken which is similar to what is used in life cycle cost estimation of solar water pumping systems. By synthesizing the cost breakdown information produced from case studies of diesel water pumping (Bengtsson & Nilsson, 2015; EMCON, 2006; Girma et al., 2015; Kelley et al., 2010; Sherrin, 2015; World Bank, 2018), the present value of maintenance and replacement costs in the life cycle of a diesel irrigation system is assumed to be three times the initial capital cost; as such  $f_{\text{gen}}$  in Equation 11 is set to 4.

In the calculation of the present value of diesel fuel costs, the discount rate  $d$  is assumed to be 5%. Diesel fuel prices at country levels obtained for 2018/2019 from the Deutsche Gesellschaft für Internationale Zusammenarbeit (GIZ, 2019) international fuel price report were used as the diesel fuel prices in year zero. Diesel prices for future years are projected under a constant price escalation rate. It is well known that fossil fuel prices are highly volatile. To address this uncertainty, our analysis included three scenarios for future diesel fuel prices. In the reference scenario, an annual price escalation rate of 2% is assumed; in the high fuel price scenario the price escalation rate is raised to 4%; in the low-fuel price scenario where the real price of diesel fuel is held constant in all future years, the escalation rate is zero.

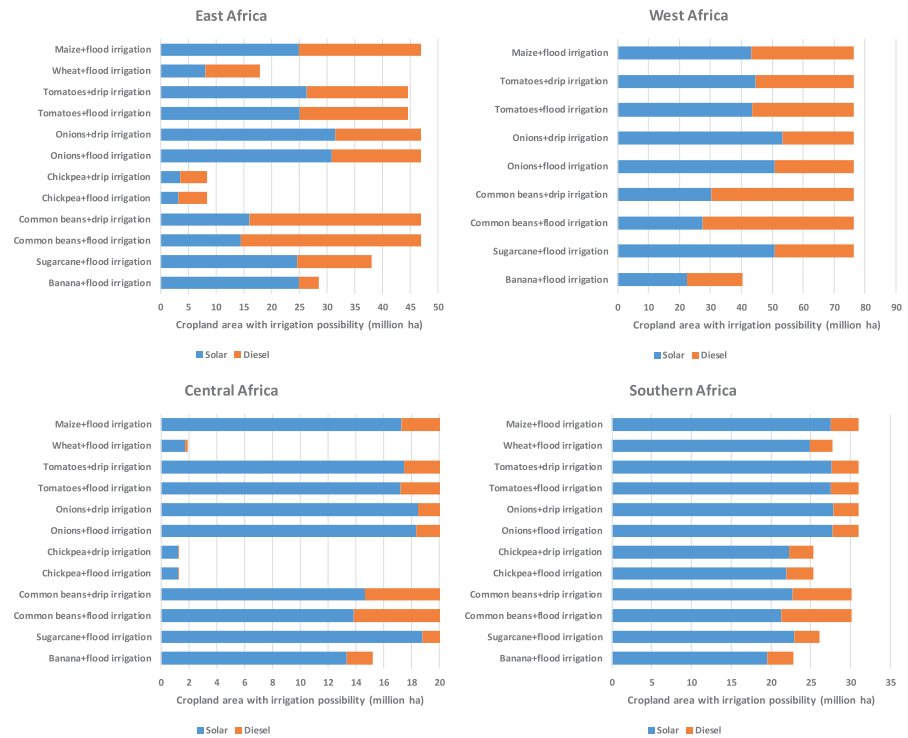
When it comes to the groundwater pumping system powered by solar PV, the information on installed cost of solar PV systems in sub-Saharan Africa is very limited. An effort to fill this knowledge gap and to collect data on the installed costs of solar energy projects in Africa is reported by the International Renewable Energy Agency (IRENA, 2016). Three types of solar PV systems: solar home systems, solar PV minigrids, and utility-scale solar PV applications were covered in the IRENA survey, and economy of scale was identified; that is, to say, unit installed cost decreases with the installed capacity of systems. Among the three types of solar PV systems, the solar home systems have capacities that are similar to those of solar PV irrigation systems investigated in this study. The unit installed cost of most surveyed solar home systems ranges between US\$5 and \$10 per watt peak, and this installed cost includes both the equipment costs for solar array and accessories (inverter, battery, and even home electronic appliances in some cases) and soft costs such as cost of installation labor, sales tax, and the overhead/profits of the service provider. Notably, in off-grid solar home systems, the battery is an essential component; its energy storage capacity ensures that the system can respond to demand in off-sunshine hours. The installed cost of the battery bank makes up a significant portion of the total installed cost and sometimes exceeds the hardware cost of the solar array. An operational characteristic that distinguishes solar PV irrigation systems from solar home systems is that the timeliness of meeting demands is less critical than for residential systems. It is thus possible to configure the solar PV power system for irrigation without a battery. If we assume a low-cost configuration of the solar PV power unit for irrigation water pumping, the installed cost of a solar PV power unit for irrigation is likely below the solar home system cost reported in the IRENA study. In addition, it is also important to note that the report was published in 2016, and cost data in the report refer to the years in which the projects were commissioned, which are even earlier than the year the report was published. Installed cost of solar PV system decreased rapidly in past decade. For example, according to U.S. NREL (National Renewable Energy Laboratory), in the United States the installed cost of solar PV residential system dropped by 63% between 2010 and 2018 from US\$7.3/Wp to 2.7 \$/Wp (Fu et al, 2018). Considering the fast pace of solar PV cost reductions and the turnaround time for data collection, analysis, and publication, it is clear that published data on solar PV costs may not reflect the latest pricing on the solar PV market.

In view of the uncertainties in the installed cost of solar PV, and in order to facilitate presenting the spatial variability in cost comparison results under this uncertainty, we calculated the breakeven installed costs of solar PV powered irrigation systems under three diesel fuel price scenarios and used it as a metric for the cost-effectiveness of solar PV irrigation relative to diesel irrigation. The breakeven installed cost is the maximum installed cost of solar PV up to which solar PV is more cost-effective than the diesel system and is calculated by rearranging Equation 9 as

$$C_{\text{installed\_BE}} = \frac{LCC_{\text{diesel}}}{1000 \cdot P_{\text{array\_STC}} \cdot f_{\text{IC}}} \quad (13)$$

where  $C_{\text{installed\_BE}}$  is the breakeven cost of the installed solar PV system (US\$/Wp). In this study,  $f_{\text{IC}}$  is set to 1.25, assuming that the installed cost accounts for 80% of the present value of the life cycle cost of the solar

(a) Escalation rate = 4%



(b) Escalation rate = 0

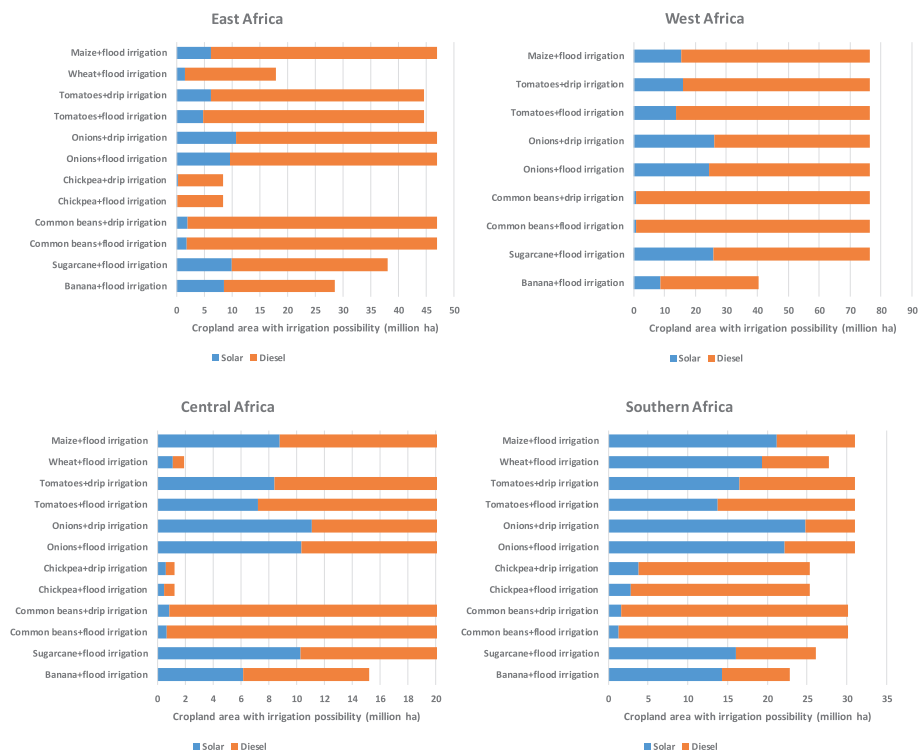
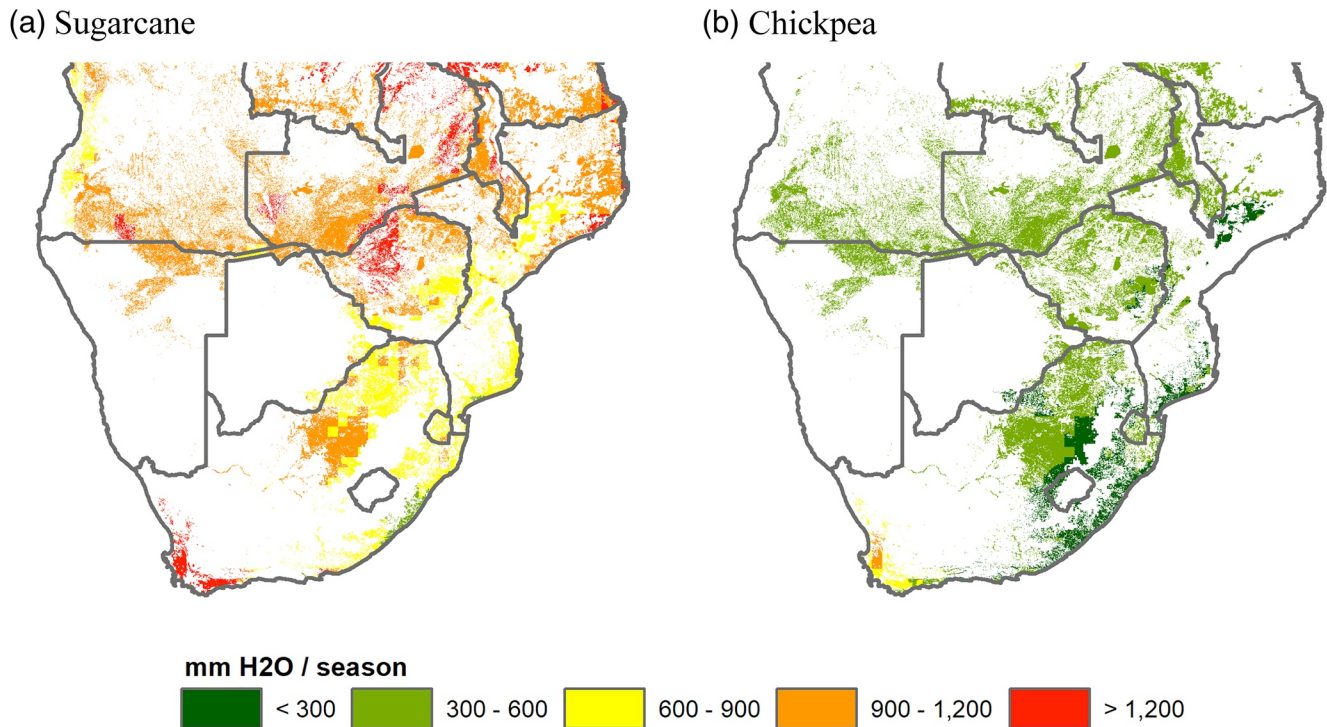


Figure 7. Cost-effective area under solar PV and diesel irrigation, under alternative diesel fuel pricing (at installed cost of solar PV of US\$2.5/Wp).



**Figure 8.** Gross irrigation water demand of sugarcane and chickpea.

PV irrigation system (Bengtsson & Nilsson, 2015; EMCON, 2006; Girma et al., 2015; Kelley et al., 2010; Sherrin, 2015; World Bank, 2018). The higher the calculated breakeven cost, the more likely it is that solar PV is more cost-effective.

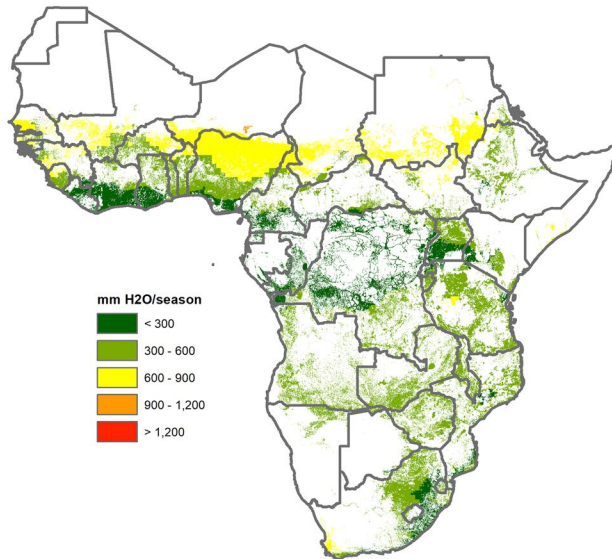
We plotted solar PV breakeven installed cost maps to encapsulate all information generated from this study. These maps can be reclassified to produce thematic maps to display the recommended energy solution for irrigation by location by taking the assigned solar PV installed cost as a class break value. In the reclassification, a pixel is labeled as “solar PV cost-effective” if the calculated breakeven installed cost for solar PV in that pixel is below the class break value, and diesel irrigation would otherwise be recommended. To be concise, we only present summarized data generated from such reclassification analysis by geographic region (i.e., East Africa, West Africa, Central Africa and Southern Africa—names of countries included in each region are shown on map in Figure 5 and added to the caption of Figure 6). By referring to solar PV costs and price trend information from the IRENA and NREL reports, three values for solar PV installed costs are assumed in the reclassification analysis: US\$2.5/Wp, US\$2/Wp, and US\$3/Wp. Using the summarized cost-effective area data, we determine the sensitivity of the cost-effective area under solar PV irrigation to the installed cost of solar PV systems. Summary data on cost-effective area of solar irrigation under alternative diesel fuel price scenarios are also presented as a demonstration of the sensitivity of the cost-effectiveness of solar PV irrigation systems to future diesel fuel prices.

#### 4. Results

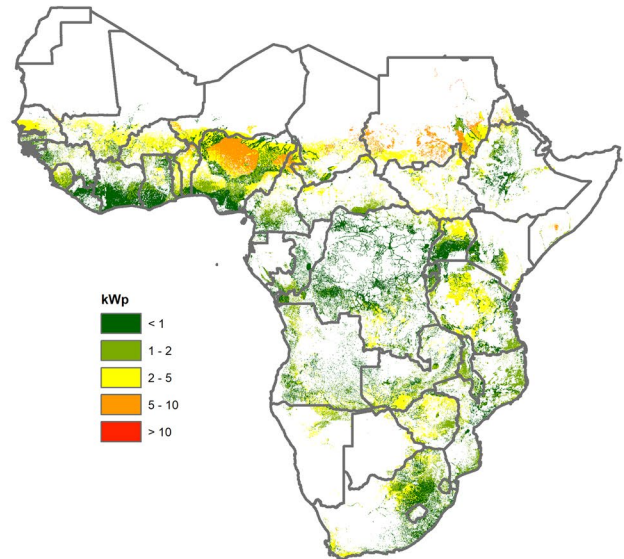
The values of several key intermediate variables: irrigation water demand, size of solar PV power system, diesel fuel consumption and power of diesel generator, calculated for the tomatoes and flood irrigation method scenario are shown in Figure 2 as an illustration of the calculations in the sizing procedure displayed in Figure 1. Moreover, the percentage share of diesel fuel cost in the life-cycle cost of the diesel power system under this crop-irrigation method scenario and the reference diesel fuel price is shown in Figure 3. It is shown that diesel fuel is the principal cost component of diesel irrigation accounting for 70%–90% of the



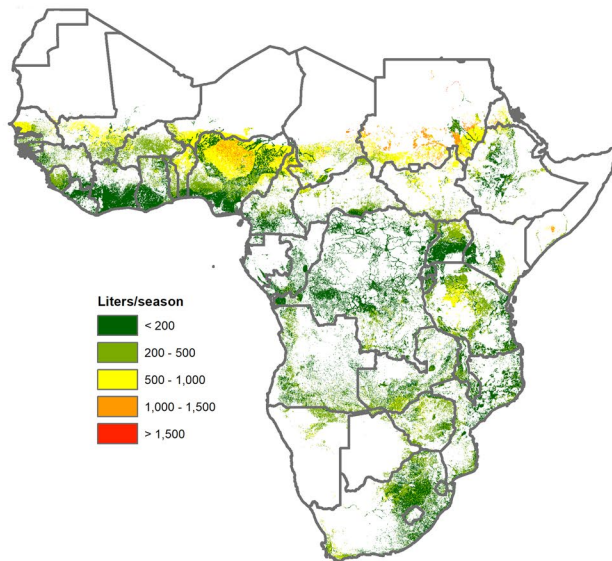
(a) Gross irrigation water demand



(b) Size of solar PV system



(c) Consumption of diesel fuel



(d) Power of diesel generator

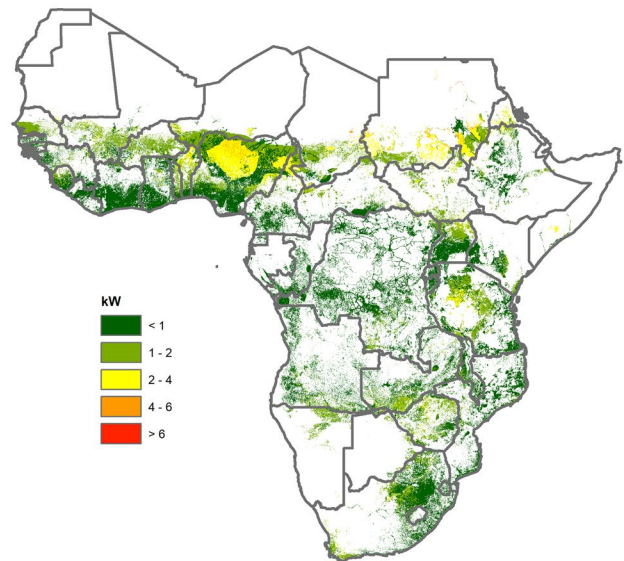


**Figure 9.** Expected values of seasonal irrigation water demand, diesel fuel consumption and required capacity of the solar PV system and power of the diesel generator derived from the Monte Carlo-based sizing calculation under the tomatoes + drip irrigation scenario.

life-cycle cost of the whole system except for a few countries with low diesel fuel prices (e.g., Sudan, Nigeria and Angola; refer to Figure 5 for diesel prices).

The solar PV breakeven installed cost maps plotted under various crop-irrigation method scenarios and under reference diesel fuel price (escalation rate of diesel fuel = 2%) are shown in Figure 4. These maps show that there is great spatial variability in calculated breakeven installed costs and that the price of diesel is undoubtedly a factor of the variability. In nearly all crop-irrigation method scenarios, low-breakeven cost values are observed at almost all locations in Sudan, Nigeria, and Angola. For the purpose of explanation, the bar chart in the right panel of Figure 5 shows the diesel fuel prices from the 2018/2019 GIZ report that were used in the study. As demonstrated by the chart, these three countries have the lowest diesel prices in sub-Saharan Africa. The diesel price in Sudan was reported at US\$0.09/liter, followed by a price of US\$0.44/liter in Angola, and US\$0.57/liter in Nigeria. Another noticeable pattern in the geographic distribution of

calculated breakeven values is that low values of breakeven installed costs of solar PV systems tend to coincide with areas with humid climate. Ghana and Côte d'Ivoire, for example, span a precipitation gradient from south to north with lower breakeven costs for solar PV found in the wetter south and higher breakeven cost values calculated in the drier north. Low breakeven values for solar PV installation are also observed in humid areas which straddle the equator in Gabon, Congo, and the Democratic Republic of the Congo. According to the definition of the breakeven installed cost, the adoption of solar irrigation is faced with more challenges in areas with low breakeven installed costs. In these areas, to be considered a more cost-effective option than diesel, the installed cost of a solar PV system often has to be below US\$2/Wp. Low solar insolation is probably a reason that leads to the unfavorableness for solar PV in these areas. By contrast, a high calculated breakeven cost tends to appear in countries with high diesel prices and in places with arid climates, two characteristics which imply better opportunities for using solar energy to power irrigation.

Figure 6 shows the cost-effective areas under the two energy solutions summarized by geographic region, as obtained through a reclassification analysis of breakeven cost maps in Figure 4. In the reclassification analysis which generated the charts in Figure 6a, the installed cost of solar PV is assumed to be US\$2.50/Wp. The largest potential of solar PV irrigation can be seen in southern Africa. Under the majority of crop-irrigation method scenarios, more than 80% of the cropland area in southern Africa is classified as solar PV cost-effective. The share of cost-effective irrigable cropland for solar PV is also high in central Africa. Although low breakeven cost values were calculated in land pixels which appear to be scattered widely in the very humid zone straddling the equator, the share of cropland in these pixels is rather low. The cost-effective area under diesel irrigation exceeds the cost-effective area under solar PV in East and West Africa. In West Africa, this is mainly because solar irrigation lacks cost-effectiveness in Nigeria, which has the largest farming in the region and low diesel cost, as noted above. In other parts of West Africa (including Senegal, Guinea, Mali, Burkina Faso, Niger, northern Côte d'Ivoire and northern Ghana), solar PV tends to be a more economical energy solution to power irrigation. In East Africa, the adoption potential of solar irrigation is concentrated in South Sudan, Eritrea, Somalia, and Tanzania.

Figures 6b and 6c show how the relative cost-effectiveness of the two energy solutions can vary with the installed cost of solar PV. Here, solar PV installed cost is set at US\$2/Wp and US\$3/Wp, respectively. As expected, the cost-effectiveness of solar PV rises with a lower solar PV installed cost (Figure 6b) and decreases as the installed cost increases (Figure 6c). The wide range of the area variable revealed in this sensitivity analysis suggests that the investment decision on energy solution selection is highly sensitive to the installed cost of solar PV. In particular, the adoption potential of solar PV surpasses that of diesel irrigation in West and East Africa when the solar PV installed cost drops to US\$2/Wp.

The solar PV breakeven installed costs calculated under the high diesel fuel price scenario (diesel fuel price escalation rate = 4%) and low diesel fuel price scenario (no change in the future diesel price) exhibit a similar pattern of spatial variability as that shown on maps in Figure 4. Figure 7 shows the summarized cost-effective areas by energy solution under the two future diesel price scenarios. These results are produced with a solar PV installed cost of US\$2.50/Wp for comparison with the graphs in Figure 4a as a demonstration of the impact of future diesel prices on the relative cost-effectiveness of groundwater irrigation systems under the two energy technologies. Not surprisingly, solar irrigation becomes more attractive in the high future diesel price scenario and less feasible in the low diesel price scenario. The change in feasible area for the two technologies again varies significantly.

In addition to spatial variability, the summarized statistics presented in Figures 6 and 7 suggest that the calculated breakeven installed costs of solar PV also possess large variability across crops. Based on share of cost-effective area, solar irrigation is found to be more suitable for irrigating sugarcane, onions, and bananas, but to perform less well in the case of chickpeas and common beans. Chickpea and common bean are two crops which have the lowest irrigation water demand, and therefore energy requirement for irrigation, among the crops included in this study. Figure 8 illustrates the difference in irrigation water demand in the irrigated production of chickpea and sugarcane in southern Africa where the cropland with suitability for chickpea is mainly located. Rather than a coincidence, the greater cost-effectiveness of solar irrigation in cultivating crops with higher irrigation water demand may be linked to the investment characteristics of the solar PV power system: solar PV investment is characterized by high upfront capital cost and in the sizing calculations we sized the solar PV system according to the irrigation demand/energy requirement in the

peak month instead of the total irrigation water/energy demand through the season. Conversely, the cost of diesel irrigation tends to escalate with irrigation water considering that the fuel cost constitutes the major part of life-cycle cost of the diesel power system (Figure 3).

Finally, it is also interesting to note that the cost-effective areas of solar and diesel groundwater pumping for drip-irrigated tomatoes, onions, chickpeas, and common beans are not significantly different from the cost-effective areas under flood-irrigated scenarios for these crops. What is behind the seemingly invariant cost-effectiveness is that, for a given irrigated crops, when there is a change in irrigation method the absolute values of estimated life-cycle costs of solar and diesel irrigation water pumping systems shift in a synchronized way, which leaves the relative cost-effectiveness of the two pumping systems more or less unchanged. The values of seasonal irrigation water demand, required capacity of the solar PV system and power of the diesel generator calculated under the tomatoes and drip irrigation scenario are plotted on maps in Figure 9 in comparison with the values of these variables plotted under the tomatoes and flood irrigation scenario in Figure 2. As is evident, drip irrigation can lead to substantial savings in water and energy consumption and downsize the requirements for both solar PV and diesel power systems. This observation is in line with conclusions from field studies by Pawar et al. (2015) and Surendran et al. (2016). The differences in absolute magnitudes of water and energy consumption/costs undoubtedly have implications for irrigation investment decisions, although it is beyond the scope of study to fully investigate such implications or address the irrigation method selection issue.

## 5. Conclusions and Discussions

In this study, we compared the cost-effectiveness of solar PV and diesel energy for groundwater pumping for irrigation in sub-Saharan Africa under a range of crop and irrigation-method scenarios. The observed cost-effectiveness of solar-powered groundwater irrigation relative to diesel-powered groundwater irrigation varies across scenarios. But overall, the results of the study show that solar PV is a promising energy solution to support groundwater-fed irrigation development. In many cases, solar energy can serve as a substitute for diesel to power groundwater pumping for irrigation more economically, particularly in the central and southern African regions. On the other hand, the fact that the calculated cost-effectiveness of solar PV is sensitive to the installed cost of solar PV and the escalation rate of diesel prices highlights the financial risk and uncertainty associated with the investment in solar powered irrigated agriculture. This is linked with the rapid development of solar energy technology and the price volatility of fossil fuels. The cost comparison analysis should thus be updated periodically in order to provide up-to-date information on cost-effectiveness which reflects the cost and pricing trends of solar energy and energy markets.

As a caveat, it is worth noting that while this study provides a first insight into the prospect of expanding groundwater irrigation under solar and diesel energy solutions in sub-Saharan Africa, it is not designed to provide a complete answer to questions such as “what is the development potential of groundwater irrigation powered by solar or diesel energy?” Irrigation development is a complex decision-process, and many factors play a role. In addition to energy costs, the economic viability of irrigation also depends on the market potential of the irrigated products, which determine revenues from the irrigated production, and costs of other inputs in crop production (e.g., seeds, fertilizers, and pesticides). There are also concerns about the groundwater overdraft risks in groundwater irrigation (Abric et al., 2011; Rodell et al., 2009; Scanlon et al., 2012). In a sound irrigation planning analysis, all these factors should be taken into account. Various approaches have been proposed to assist in strategic irrigation planning analysis in sub-Saharan Africa. For example, there are studies that used GIS (Geographic Information System) tools and MCE (Multi Criteria Evaluation) techniques to score land suitability for irrigation and delineated area with irrigation development potential (Berhanu & Hatiye, 2020; Schmitter et al., 2018; Worqlul et al., 2017). Xie et al. (2014, 2017, 2021) developed an integrated modeling framework which combines the use of GIS land suitability analysis, hydrological/crop simulation and economic modeling tools with cost-benefit and sustainability of irrigation development being evaluated explicitly. The data developed in this cost comparison study can be used to augment these analyses by introducing additional suitability criteria in MCE analysis and incorporating a decision process of energy solution selection in Xie et al. (2021)'s model to generate enhanced estimates of groundwater irrigation development potential under different energy solutions. This constitutes an interesting topic for future research.



## Data Availability Statement

All the data used in the analysis are publicly available and can be accessed via supporting information (Table S2). GIS source data files of breakeven cost maps that are shown in Figure 4 and generated under two alternative diesel fuel price scenarios are deposited to <https://doi.org/10.7910/DVN/TI7VYF>.

## Acknowledgments

This project is part of the CGIAR Research Program on Water, Land and Ecosystems (WLE). It is supported by CGIAR Fund Donors (<http://www.cgiar.org/who-we-are/cgiar-fund/fund-donors-2>). The research was conducted by a team of scientists based at the International Food Policy Research Institute (IFPRI) and at Daffodil International University. We also thank Dr. Petra Schmitter at the International Water Management Institute (IWMI) for her constructive comments.

## References

- Abric, S., Sonou, M., Augeard, B., Onimus, F., Durlin, D., Soumaila, A., et al. (2011). *Lessons learned in the development of smallholder private irrigation for high-value crops in West Africa*. World Bank.
- Abu-Aligah, M. (2011). Design of photovoltaic water pumping system and compare it with diesel powered pump. *Jordan Journal of Mechanical and Industrial Engineering*, 5(3), 273–280.
- Allen, R. G., Pereira, L. S., Raes, D., & Smith, M. (1998). In: Crop evapotranspiration—Guidelines for Computing Crop water requirements—FAO Irrigation and drainage paper 56. Rome: FAO.
- Barrueto Guzmán, A., Barraza Vicencio, R., Ardila-Rey, J., Núñez Ahumada, E., González Araya, A., & Arancibia Moreno, G. (2018). A cost-effective methodology for sizing solar PV systems for existing irrigation facilities in Chile. *Energies*, 11(7), 1853.
- Baumann, E., Ball, P., & Beyene, A. (2005). *Rationalization of drilling operations in Tanzania*. In Review of the borehole drilling Sector in Tanzania (St. Gallen: Rural water supply network).
- Belaud, G., Mateos, L., Aliod, R., Buisson, M.-C., Faci, E., Gendre, S., et al. (2020). Irrigation and energy: Issues and challenges. *Irrigation and Drainage*, 69(Supp. 1), 177–185. <https://onlinelibrary.wiley.com/doi/epdf/10.1002/ird.2343>
- Bengtsson, N., & Nilsson, J. (2015). *Solar water Pumping for irrigation: Case Study of the Kilimanjaro region*. Independent Thesis.
- Berhanu, K. G., & Hatiye, S. D. (2020). Identification of groundwater potential zones using proxy data: Case study of Megech watershed, Ethiopia. *Journal of Hydrology: Regional Studies*, 28, 100676.
- Blimpo Moussa, P., & Cosgrove-Davies, M. (2019). *Electricity access in sub-Saharan Africa: Uptake, reliability, and complementary factors for economic impact Africa development forum*. Washington, DC: World Bank. <https://openknowledge.worldbank.org/handle/10986/31333>
- Bonsor, H. C., & MacDonald, A. M. (2011). *An initial estimate of depth to groundwater across Africa, Groundwater Science Programme Open Report OR/11/067*. British Geological Survey.
- Borehole Water Association of Southern Africa (2020). <https://bwa.co.za/laypersons-guide>
- Brouwer, C., Prins, K., & Heibloem, M. (1989). *Irrigation water management: Irrigation scheduling*. Training manual no. 4. Rome: FAO. <http://www.fao.org/tempref/agl/AGLW/fwm/Manual5.pdf>
- Burney, J., Woltering, L., Burke, M., Naylor, R., & Pasternak, D. (2010). Solar-powered drip irrigation enhances food security in the Sudano-Sahel. *Proceedings of the National Academy of Sciences*, 107(5), 1848–1853. <https://doi.org/10.1073/pnas.0909678107>
- Burney, J. A., Naylor, R. L., & Postel, S. L. (2013). The case for distributed irrigation as a development priority in sub-Saharan Africa. *Proceedings of the National Academy of Sciences*, 110(31), 12513–12517.
- Cobbing, J., & Hiller, B. (2019). *Waking a sleeping giant: Realizing the potential of groundwater in Sub-Saharan Africa*, 122, 597–613. <https://doi.org/10.1016/j.worlddev.2019.06.024>
- Cuadros, F., López-Rodríguez, F., Marcos, A., & Coello, J. (2004). A procedure to size solar-powered irrigation (photoirrigation) schemes. *Solar Energy*, 76(4), 465–473.
- de Fraiture, C., & Giordano, M. (2014). Small private irrigation: a thriving but overlooked sector. *Agricultural Water Management*, 131, 167–174.
- de Graaf, I. E., van Beek, R. L., Gleeson, T., Moosdorf, N., Schmitz, O., Sutanudjaja, E. H., et al. (2017). A global-scale two-layer transient groundwater model: Development and application to groundwater depletion. *Advances in Water Resources*, 102, 53–67.
- Domènech, L. (2015). Improving irrigation access to combat food insecurity and undernutrition: A review. *Global Food Security*, 6, 24–33. EMCON (2006). *Feasibility assessment for the replacement of diesel water pumps with solar water pumps*. Windhoek, Namibia: UNDP.
- FAO (1997). *Irrigation potential in Africa: A basin approach*. FAO land and water bull. Rome: FAO.
- FAO (2016). *Aquastat*. Rome: FAO. <http://www.fao.org/land-water/databases-and-software/aquastat/en/>
- FAO (2020). *Smallholders dataportrait*. Rome: FAO <http://www.fao.org/family-farming/data-sources/dataportrait/farm-size/en/>
- FAO and ECA (2018). *Regional overview of food security and nutrition. Addressing the threat from climate variability and extremes for food security and nutrition*. Accra: FAO.
- Fischer, G., Nachtergaele, F. O., Prieler, S., Teixeira, E., Tóth, G., Van Velthuizen, H., et al. (2012). *Global agro-ecological zones (GAEZ v3.0)—Model documentation*. Laxenburg, Austria: IIASA and Rome: FAO
- Fritz, S., See, L., McCallum, I., You, L., Bun, A., Moltchanova, E., et al. (2015). Mapping global cropland and field size. *Global Change Biology*, 21(5), 1980–1992
- Fu, R., Feldman, D. J., & Margolis, R. M. (2018). *US solar photovoltaic system cost benchmark: Q1 2018 Technical report NREL/TP-6A20-72399*. Golden, CO: National Renewable Energy Lab.
- Funk, C., Peterson, P., Landsfeld, M., Pedreros, D., Verdin, J., Shukla, S., et al. (2015). The climate hazards infrared precipitation with stations—A new environmental record for monitoring extremes. *Scientific Data*, 2(1), 1–21.
- Girma, M., Assefa, A., & Molinas, M. (2015). Feasibility study of a solar photovoltaic water pumping system for rural Ethiopia. *AIMS Environment Science*, 2(3), 697–717.
- GIZ (2019). *International Fuel Prices 2018/19*. Eschborn, Germany: German Corporation for International Cooperation. [http://sutp.transport-nama.org/files/contents/documents/resources/K\\_International%20Fuel%20Prices/GIZ\\_SUTP\\_IFP\\_2018-19\\_EN.pdf](http://sutp.transport-nama.org/files/contents/documents/resources/K_International%20Fuel%20Prices/GIZ_SUTP_IFP_2018-19_EN.pdf)
- Harris, I., Jones, P. D., Osborn, T. J., & Lister, D. H. (2014). Updated high-resolution grids of monthly climatic observations—the CRU TS3.10 Dataset. *International Journal of Climatology*, 34(3), 623–642.
- Hartmann, J., & Moosdorf, N. (2012). The new global lithological map database GLiM: A representation of rock properties at the Earth surface. *Geochemistry, Geophysics, Geosystems*, 13(12).
- Hartung, H., & Pluschke, L. (2018). *The benefits and risks of solar-powered irrigation—a global overview*. Rome: FAO.
- Hossain, M. A., Hassan, M. S., Mottalib, M. A., & Hossain, M. (2015). Feasibility of solar pump for sustainable irrigation in Bangladesh. *International Journal of Energy and Environmental Engineering*, 6(2), 147–155.
- Huld, T., Müller, R., & Gambardella, A. (2012). A new solar radiation database for estimating PV performance in Europe and Africa. *Solar Energy*, 86(6), 1803–1815.



- IRENA (2016). *Solar PV in Africa: Costs and markets*. <https://www.irena.org/publications/2016/Sep/Solar-PV-in-Africa-Costs-and-Markets>
- Kelley, L. C., Gilbertson, E., Sheikh, A., Eppinger, S. D., & Dubowsky, S. (2010). On the feasibility of solar-powered irrigation. *Renewable and Sustainable Energy Reviews*, *14*(9), 2669–2682.
- Langarita, R., Chóliz, J. S., Sarasa, C., Duarte, R., & Jiménez, S. (2017). Electricity costs in irrigated agriculture: a case study for an irrigation scheme in Spain. *Renewable and Sustainable Energy Reviews*, *68*, 1008–1019.
- Lorenzo, C., Almeida, R. H., Martínez-Núñez, M., Narvarte, L., & Carrasco, L. M. (2018). Economic assessment of large power photovoltaic irrigation systems in the *ECOWAS Region Energy*, *155*, 992–1003.
- Lowder, S. K., Scoet, J., & Raney, T. (2016). The number, size, and distribution of farms, smallholder farms, and family farms worldwide. *World Development*, *87*, 16–29.
- MacDonald, A. M., Bonsor, H. C., Ó Dochartaigh, B. É., & Taylor, R. G. (2012). Quantitative maps of groundwater resources in Africa. *Environmental Research Letters*, *7*(2), 024009.
- MacDonald, A. M., Ó Dochartaigh, B. É., Calow, R. C., Shalabi, Y., Selah, K., & Merrett, S. (2009). Mapping groundwater development costs for the transboundary Western Aquifer Basin, Palestine/Israel. *Hydrogeology Journal*, *17*(7), 1579.
- Njuki, J., Waithanji, E., Sakwa, B., Kariuki, J., Mukewa, E., & Ngige, J. (2014). A qualitative assessment of gender and irrigation technology in Kenya and Tanzania. *Gender, Technology and Development*, *18*(3), 303–340.
- Pawar, N., Bishnoi, D. K., Singh, M., & Dhillon, A. (2015). Comparative economic analysis of drip irrigation vis-a-vis flood irrigation system on productivity of Bt. cotton in Haryana. *Agricultural Science Digest*, *35*(4), 300–303.
- Phocaides, A. (2007). *Handbook on pressurized irrigation techniques*. Rome: FAO.
- Postel, S., Polak, P., Gonzales, F., & Keller, J. (2001). Drip irrigation for small farmers: A new initiative to alleviate hunger and poverty. *Water International*, *26*(1), 3–13.
- Rodell, M., Velicogna, I., & Famiglietti, J. S. (2009). Satellite-based estimates of groundwater depletion in India. *Nature*, *460*(7258), 999–1002.
- Scanlon, B. R., Faunt, C. C., Longuevergne, L., Reedy, R. C., Alley, W. M., McGuire, V. L., et al. (2012). Groundwater depletion and sustainability of irrigation in the US High Plains and Central Valley. *Proceedings of the National Academy of Sciences of the United States of America*, *109*(24), 9320–9325.
- Schmitter, P., Kibret, K. S., Lefore, N., & Barron, J. (2018). Suitability mapping framework for solar photovoltaic pumps for smallholder farmers in sub-Saharan Africa. *Applied Geography*, *94*, 41–57.
- Sherrin, A. R. (2015). *Water use and system reliability under diesel generator and solar photovoltaic powered pumping systems: A case study of Solla Togo*. Master's thesis Michigan Technological University.
- Short, W., Packey, D. J., & Holt, T. (1995). *A manual for the economic evaluation of energy efficiency and renewable energy technologies*. Technical Report NREL/TP-462-5173. National Renewable Energy Lab.
- Siebert, S., Burke, J., Faures, J. M., Frenken, K., Hoogeveen, J., Döll, P., et al. (2010). Groundwater use for irrigation—a global inventory. *Hydrology and Earth System Sciences*, *14*(10), 1863–1880.
- Smith, M. (1992). *Cropwat – a computer program for irrigation planning and management, Irrigation and drainage paper 46*. Rome: FAO.
- Surendran, U., Jayakumar, M., & Marimuthu, S. (2016). Low cost drip irrigation: Impact on sugarcane yield, water and energy saving in semiarid tropical agro ecosystem in India. *The Science of the Total Environment*, *573*, 1430–1440.
- Szabó, S., Bódis, K., Huld, T., & Moner-Girona, M. (2011). Energy solutions in rural Africa: Mapping electrification costs of distributed solar and diesel generation versus grid extension. *Environmental Research Letters*, *6*(3), 034002.
- Tarjuelo, J. M., Rodríguez-Díaz, J. A., Abadía, R., Camacho, E., Rocamora, C., & Moreno, M. A. (2015). Efficient water and energy use in irrigation modernization: Lessons from Spanish case studies. *Proceedings of the ICE - Agricultural Water Management*, *162*, 67–77.
- Theis, C. V. (1935). The relation between the lowering of the piezometric surface and the rate and duration of discharge of a well using ground-water storage. *Eos, Transactions American Geophysical Union*, *16*(2), 519–524. <https://doi.org/10.1029/TR016i002p00519>
- Villholth, K. G. (2013). Groundwater irrigation for smallholders in Sub-Saharan Africa—a synthesis of current knowledge to guide sustainable outcomes. *Water Bar International Series*, *38*(4), 369–391.
- Woltering, L., Pasternak, D., & Ndjeunga, J. (2011). The African market garden: the development of a low-pressure drip irrigation system for smallholders in the Sudano Sahel. *Irrigation and Drainage*, *60*(5), 613–621.
- World Bank (2018). *Solar pumping: The basics (English)*. Washington, DC: World Bank. <http://documents.worldbank.org/curated/en/880931517231654485/Solar-pumping-the-basics>
- Worqlul, A. W., Jeong, J., Dile, Y. T., Osorio, J., Schmitter, P., Gerik, T., et al. (2017). Assessing potential land suitable for surface irrigation using groundwater in Ethiopia. *Applied Geography*, *85*, 1–13.
- Xie, H., You, L., Dile, Y. T., Worqlul, A. W., Bizimana, J. C., Srinivasan, R., Richardson, J. W., et al. (2021). Mapping development potential of dry-season small-scale irrigation in Sub-Saharan African countries under joint biophysical and economic constraints—An agent-based modeling approach with an application to Ethiopia. *Agricultural Office Systems*, *186*, 102987.
- Xie, H., You, L., & Takeshima, H. (2017). Invest in small-scale irrigated agriculture: A national assessment on potential to expand small-scale irrigation in Nigeria. *Agricultural Water Manage*, *193*, 251–264.
- Xie, H., You, L., Wielgosz, B., & Ringler, C. (2014). Estimating the potential for expanding smallholder irrigation in Sub-Saharan Africa. *Agricultural Water Manage*, *131*, 183–193.